ADABOOST-BASED LOCAL-FOREST ADVERSARIAL LEARNING FOR IMBALANCED DOMAIN ADAPTATION

Anonymous authors
Paper under double-blind review

ABSTRACT

Class imbalance poses a significant challenge in unsupervised domain adaptation (UDA). We propose Adaboost-based Local-Forest Adversarial Learning (ALFAL), a framework that leverages sample-wise label matching rates to guide both adaptive sampling and interpolation-based generation. ALFADA first samples informative instances and constructs a local discriminative forest (LDF) via clustering to enable fine-grained regional alignment on the basis of the global discriminator in the framework of domain adversarial learning. To further enhance adaptation for minority classes, a Boosted Pairwise Interpolation Generator (BPIG) synthesizes interpolation samples between high-weight source and confident target instances. These auxiliary samples are optimized through an adversarial learning-based exploration mechanics to explore challenging regions. Experiments demonstrate that ALFADA consistently outperforms existing state-of-the-art methods on imbalanced domain adaptation benchmarks.

1 INTRODUCTION

Unsupervised Domain Adaptation (UDA) aims to transfer knowledge from a labeled source domain to an unlabeled target domain by mitigating the distributional discrepancy between them. While recent UDA techniques (Ganin & Lempitsky, 2016; Long et al., 2018) have achieved promising results under the assumption of balanced class distributions, this assumption is often violated in real-world scenarios. Both the source and target domains frequently exhibit significant class imbalance, where a few categories dominate the data while others remain under-represented. This exacerbates alignment difficulty and leads to degraded performance on minority classes, a problem referred to as Class-Imbalanced Domain Adaptation (CDA) (Tan et al., 2020; Wu et al., 2019b).

To address this, existing works have primarily followed two directions: pseudo-label-based self-training and data augmentation. Pseudo-labeling methods (Tan et al., 2020; Jiang et al., 2020; Prabhu et al., 2021) generate class predictions on unlabeled target samples and retrain the model in a self-supervised fashion. Some methods incorporate class-aware weighting or region-specific alignment based on the pseudo-label (Alcover-Couso et al., 2025; Liu et al., 2023b). However, these methods often rely on static or pre-defined alignment structures, limiting their ability to adaptively emphasize hard or minority-class regions during training.

To complement pseudo-labeling, a growing body of research has focused on data augmentation, especially for minority classes. Adversarial augmentation methods (Miyato et al., 2018; Shu et al., 2018) and sample interpolation approaches (Shi et al., 2022b) have shown that generating synthetic samples along decision boundaries can enrich target domain coverage and enhance classifier robustness. Pairwise Adversarial Training (PAT) (Shi et al., 2022b), for example, interpolates between a source and a target sample of the same class to generate informative intermediate samples. However, most existing augmentation methods do not explicitly identify alignment difficulty or underperforming regions, and often assume correct sample pairing which may not hold under pseudo-label noise and distributional shift.

To bridge these gaps, we propose a unified framework named Adaboost-based Local-Forest Adversarial Domain Adaptation (ALFADA), which jointly addresses class imbalance, pseudo-label noise, and fine-grained domain misalignment. ALFADA is composed of three tightly coupled components that work synergistically to enhance adaptation performance under class-imbalanced settings.

First, we introduce an adaptive sample reweighting mechanism inspired by AdaBoost. In each epoch of the training, we estimate the per-class matching error rates (MER) to reflect the alignment quality across domains. These rates are used to dynamically assign weights to individual samples, emphasizing hard-to-align or minority-class instances so as to push the model to allocate more attention to informative and underrepresented samples.

Building upon the weighted sampling, we then construct a local discriminative forest (LDF) on the basis of the framework of adversarial domain adaptation. Instead of relying solely on a single global domain discriminator, ALFADA partitions the feature space into multiple clusters and trains a separate local domain discriminator adaptively for each cluster alongside the global one. This forest-like structure captures fine-grained regional discrepancies between domains and preserves local semantic consistency, which is especially beneficial for the alignment of rare categories that may otherwise be overwhelmed by dominant classes in global alignment.

Finally, to further enhance the feature space coverage of minority classes, we propose a Boosted Pairwise Interpolation Generator (BPIG). BPIG synthesizes new samples by interpolating between high-weighted source instances and confident target samples of the same predicted class. These interpolated samples serve as bridges between sparse regions in the joint feature space. Furthermore, we design an adversarial learning-based exploration mechanics to optimize the generated samples in order to explore the challenging regions. BPIG ensures that the generated samples lie near class boundaries and guide the classifier to learn more discriminative decision surfaces, particularly for underrepresented or ambiguous classes.

In summary, our contributions are threefold:

- Introduce an adaptive reweighting mechanism that guides all stages of training to focus on minority and/or hard-to-align samples.
- Construct a local discriminative forest via adaptive sampling and clustering, leveraging ensemble effects to realize fine-grained feature alignment and prevent overfitting towards the majority classes.
- Propose a boosted interpolation generator that synthesizes informative source-target samples to densify low-density regions and enhance minority-class learning.

2 Related work

Class-Imbalanced Domain Adaptation. Class-imbalanced domain adaptation (CDA) poses additional challenges due to biased prediction toward frequent classes. Early works like COAL (Tan et al., 2020) and Implicit Class Conditioning (Jiang et al., 2020) leverage pseudo-labels to enforce class balance during self-training. ACE (Wu et al., 2019b) introduces asymmetrical alignment losses, while SENTRY (Prabhu et al., 2021) uses consistency regularization to filter noisy pseudo-labels. Recent studies such as WUDA (Liu et al., 2023a) refines weighting mechanisms or fusion strategies to better handle imbalance. GBW (Huang et al., 2023), dynamically weight classes by gradient magnitude. In parallel, advanced reweighting techniques have been proposed to tackle class imbalance. For example, Guo et al. (Guo et al., 2022) formulate sample weighting as an optimal transport problem to directly balance class distributions without expensive bilevel optimization. However, all these approaches heavily rely on pseudo-label quality, which is particularly unreliable for rare classes.

Multi-discriminator adversarial learning Adversarial-based UDA frameworks like DANN (Ganin & Lempitsky, 2016) focus on marginal alignment using a global domain discriminator. MADA (Pei et al., 2018) extends this idea by employing class-wise discriminators to capture conditional distributions. COT (Liu et al., 2023b) uses clustering and optimal transport to align cluster-level prototypes. To better address class-specific misalignment, some works introduce fine-grained alignment strategies. For example, CaCo (Huang et al., 2022) employs category-aware contrastive objectives to preserve class-wise feature separation during alignment, and an attention-based class-conditioned aligner (ACIA) (Belal et al., 2025) for multi-source DA was proposed to specifically improve alignment of minority classes in object detection. Such approaches highlight the benefit of local discriminators focused on challenging regions, though they are not yet widely integrated into standard UDA pipelines.

Data Augmentation and Sample Generation. Data augmentation plays a key role in enhancing target coverage, especially for rare categories. SMOTE-style oversampling has been widely applied in traditional long-tailed learning, but less so in UDA. Virtual Adversarial Training (VAT) (Miyato et al., 2018; Shu et al., 2018) introduces input perturbations to enforce smoothness. PAT (Shi et al., 2022b) advances this by generating synthetic samples through source–target interpolation. Recently, generative data augmentation has made progress by leveraging large pre-trained models to bridge domains. For instance, DoGE (Wang et al., 2024) uses a diffusion-based strategy to generate target-style synthetic samples by encoding the source–target domain gap, yielding performance gains without requiring explicit source-target pairs. However, these modern augmentation techniques either assume accurate source–target pairing or ignore region-specific alignment difficulty.

3 METHODOLOGY

3.1 PROBLEM SETUP AND FRAMEWORK OVERVIEW

We address the problem of *unsupervised domain adaptation (UDA)* under *class imbalance*, where both the source and target domains exhibit long-tailed label distributions. Formally, let the labeled source domain be denoted as $\mathcal{D}_s = \{(\boldsymbol{x}_i^s, y_i^s)\}_{i=1}^{N_s}$, and the unlabeled target domain as $\mathcal{D}_t = \{\boldsymbol{x}_j^t\}_{j=1}^{N_t}$, where $y_i^s \in \{1, \ldots, C\}$ and C is the total number of categories. The goal is to learn a feature extractor $g(\cdot)$ and classifier $f(\cdot)$ such that $f(g(\boldsymbol{x}_j^t))$ yields accurate predictions for target samples.

The ALFADA framework consists of five key components: Feature Extractor (g): Maps both source and target samples into a shared feature space; Local discriminative forest: Constructs K local domain discriminators via weighted K-means clustering, supplemented by a global discriminator; Classifier (f): Provides class predictions for both source supervision and target pseudo-labeling. An overview of the proposed framework is shown in Figure 1.

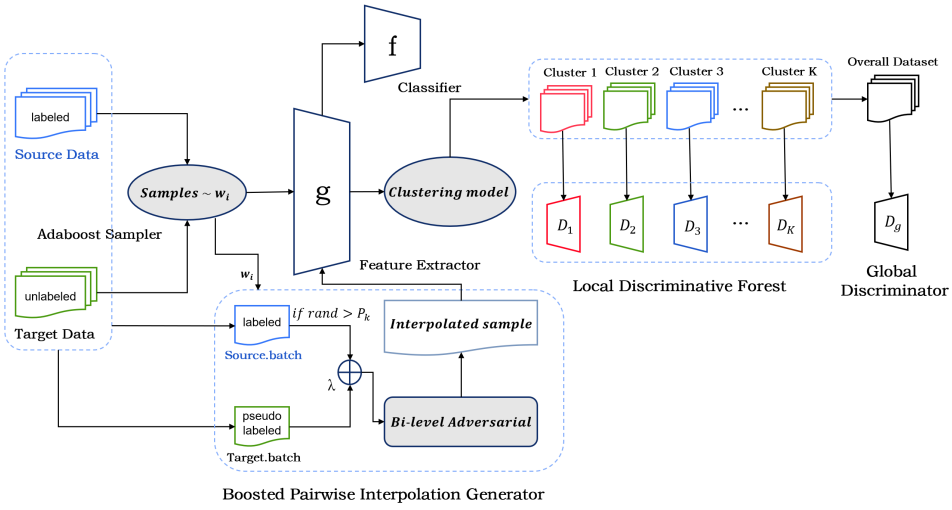

Figure 1: Overall architecture of the ALFADA framework.

3.2 ADAPTIVE MATCHING ERROR RATE SAMPLING

To effectively highlight hard-to-align and minority-class samples under class imbalance, we introduce an adaptive *matching error rate*–based weighting scheme. This mechanism serves as the foundation for weighted sampling and downstream clustered domain alignment.

3.2.1 PSEUDO-LABEL ASSIGNMENT THRESHOLD

First, we define the overall sample set $\mathcal{D} = \{(\boldsymbol{x}_i, y_i^{\text{match}}, d_i)\}_{i=1}^N$ where $\boldsymbol{x}_i$ is the input sample, y_i^{match} is the corresponding matching label, and $d_i \in \{0, 1\}$ indicates the domain (0 for source, 1 for target). The definition of y_i^{match} depends on the domain to which $\boldsymbol{x}_i$ belongs. For source domain samples, y_i^{match} is simply the ground-truth label y_i^s. For target domain samples, we rely on pseudo-labels $\hat{y}_i^t$ predicted by the classifier trained in the previous epoch. To maintain a stable training, only target samples with pseudo-label confidence above a fixed threshold τ are included. Specifically, we set:

$$y_i^{\text{match}} = \begin{cases} y_i^s & \text{if } \boldsymbol{x}_i \in \mathcal{D}_s \\ \hat{y}_i^t & \text{if } \boldsymbol{x}_i \in \mathcal{D}_t \text{ and } p(\hat{y}_i^t) \geq \tau \end{cases}$$

Target samples with confidence below τ are excluded from matching rate computation and weight updates in order to rule out the noise in the pseudo-labels.

3.2.2 DEFINITION OF MATCHING ERROR RATE

We define the *matching error rate* (MER) ε_c for each class $c \in \{1, \ldots, C\}$ as follows:

$$\varepsilon_c = \frac{\sum_{i: y_i^{\text{match}} = c} w_i \cdot \mathbb{I}(f(g(\boldsymbol{x}_i)) \neq y_i^{\text{match}})}{\sum_{i: y_i^{\text{match}} = c} w_i} \tag{1}$$

Here, $f(g(\boldsymbol{x}_i))$ denotes the predicted class for input $\boldsymbol{x}_i$, w_i is the current sample weight, and $\mathbb{I}(\cdot)$ is the indicator function.

3.2.3 ADAPTIVE SAMPLING

We initialize all weights uniformly as $w_i^{(0)} = 1/N$ at the beginning and normalize after each update to ensure that $\sum_i w_i = 1$. Once the matching rate ε_c is computed at t-th epoch, we derive a class-level coefficient α_c using an Adaboost-style formulation:

$$\alpha_c = \frac{1}{2} \ln \left(\frac{1 - \varepsilon_c}{\varepsilon_c} \right) \tag{2}$$

Based on α_c, we update the adaptive weight for each class via:

$$w_i^{(t+1)} = w_i^{(t)} \cdot \exp \left(\alpha_{y_i^{\text{match}}} \cdot \mathbb{I}(f(g(\boldsymbol{x}_i)) \neq y_i^{\text{match}}) \right) \tag{3}$$

This update rule increases the weight w_i for samples that are misclassified, especially those belonging to harder classes with larger α_c. We initialize all weights uniformly as $w_i^{(0)} = 1/N$ and normalize after each update to ensure that $\sum_i w_i = 1$.

Then we use these adaptive weights to construct a rebalanced training dataset $\mathcal{D}_w$ through sampling with replacement. Each sample $\boldsymbol{x}_i$ is selected with probability w_i:

$$P(\boldsymbol{x}_i \in \mathcal{D}_w) = w_i$$

This mechanism implicitly amplifies the contribution of underrepresented and hard-to-classify samples. As a result, the constructed dataset $\mathcal{D}_w$ better reflects the class distribution difficulties and provides a more informative basis for downstream clustering and adversarial training.

3.3 LOCAL DISCRIMINATIVE FOREST

To capture fine-grained domain discrepancies under class imbalance, we introduce a Local Discriminative Forest (LDF) on the basis of DANN. The LDF consists of multiple local domain discriminators, each trained on a specific sub-region of the feature space. This design compensates for the limitations of a single global discriminator, which tends to align dominant modes of the distribution while overlooking minority-class features.

The domain discriminator forest consists of K independent sub-domain discriminators $\{D_1, D_2, \ldots, D_K\}$ and a global discriminator D_{global}. Each sub-domain discriminator D_i is trained on a distinct dataset $\mathcal{C}_i$, sampled by weighted K-means clustering.

3.3.1 MER-WEIGHTED CLUSTERING

To enable fine-grained domain alignment, we partition the weighted training set $\mathcal{D}_w$ into K subdomains using a weighted K-means algorithm. Each sample $\boldsymbol{x}_i$ is represented by its feature $\boldsymbol{z}_i = g(\boldsymbol{x}_i)$ and associated adaptive weight w_i from Section 2.2. By incorporating w_i into the clustering process, samples from minority classes or hard-to-align regions exert greater influence on cluster formation.

We first initialize K cluster centroids $\{\boldsymbol{\mu}_1^{(0)}, \ldots, \boldsymbol{\mu}_K^{(0)}\}$ by sampling features from $\mathcal{D}_w$ with probability proportional to w_i. This encourages initialization near informative, underrepresented regions.

Clustering proceeds by alternately assigning each $\boldsymbol{z}_i$ to the nearest centroid based on weighted distance

$$\text{dist}_w(\boldsymbol{z}_i, \boldsymbol{\mu}_k^{(p)}) = w_i \cdot \|\boldsymbol{z}_i - \boldsymbol{\mu}_k^{(p)}\|_2^2, \tag{4}$$

and updating each centroid as the weighted average of its assigned features:

$$\boldsymbol{\mu}_k^{(p+1)} = \frac{\sum_{\boldsymbol{z}_i \in \mathcal{C}_k} w_i \cdot \boldsymbol{z}_i}{\sum_{\boldsymbol{z}_i \in \mathcal{C}_k} w_i}. \tag{5}$$

The procedure terminates after a fixed number of iterations T_{cluster} or when all centroid updates fall below a threshold ϵ.

The resulting partition $\{\mathcal{C}_1, \ldots, \mathcal{C}_K\}$ defines K local feature regions. Each cluster $\mathcal{C}_k$ is assigned a dedicated domain discriminator D_k, responsible for aligning source and target distributions within that region. To ensure that the local domain discriminators remain aligned with the current feature distribution and balance the precision-efficiency trade-off, we perform this weighted clustering every T epochs.

3.3.2 ADAPTIVE DOMAIN ALIGNMENT

Once the updated clusters $\{\mathcal{C}_1, \ldots, \mathcal{C}_K\}$ are formed, we re-initialize the local discriminators $\{D_k\}_{k=1}^K$, each of which is trained to distinguish source from target samples within its assigned cluster. Since some subdomains may be more difficult to align than others (e.g., those dominated by minority classes or exhibiting more shift), we assign each D_k an adaptive importance weight based on its domain classification performance.

Each local discriminator D_k is trained to distinguish source from target samples within its corresponding cluster $\mathcal{C}_k$, using a binary cross-entropy loss defined as:

$$\mathcal{L}_{\text{local},k} = -\frac{1}{N_k} \sum_{i \in \mathcal{C}_k} \Big[d_i \log(D_k(\boldsymbol{z}_i)) + (1 - d_i) \log(1 - D_k(\boldsymbol{z}_i)) \Big] \tag{6}$$

where $d_i \in \{0, 1\}$ denotes the domain label (0 for source, 1 for target), N_k is the sample size of $\mathcal{C}_k$ and $D_k(\boldsymbol{z}_i)$ is the predicted domain probability output by the k-th local discriminator.

To avoid overfitting to localized patterns and ensure global distribution alignment, we keep the original global domain discriminator D_{global}, which is trained on a overall dataset $\mathcal{D}_w$ at this epoch. The resulted loss function is defined as:

$$\mathcal{L}_{\text{global}} = -\frac{1}{N} \sum_{i=1}^{N} \Big[d_i \log(\hat{d}_{i,\text{global}}) + (1 - d_i) \log(1 - \hat{d}_{i,\text{global}}) \Big] \tag{7}$$

where $N = \sum_{k=1}^K N_k$ and $\hat{d}_{i,\text{global}} = D_{\text{global}}(\boldsymbol{z}_i)$, which is the predicted domain label probability by D_{global}.

Specifically, in order to direct the model's focus toward more challenging areas, we evaluate each local discriminator D_k on a validation subset $\mathcal{V}_k \subseteq \mathcal{C}_k$ and compute its domain error rate:

$$\delta_k = \frac{1}{|\mathcal{V}_k|} \sum_{i \in \mathcal{V}_k} \mathbb{I}(D_k(\boldsymbol{z}_i) \neq d_i), \tag{8}$$

where $d_i \in \{0, 1\}$ is the ground-truth domain label (source or target) of sample $\boldsymbol{x}_i$. The corresponding importance weight β_k is then computed via:

$$\beta_k = \frac{1}{2} \ln \left(\frac{1 - \delta_k}{\delta_k} \right). \tag{9}$$

Intuitively, regions with high δ_k represent under-adapted subdomains, which should contribute more strongly to the overall alignment process.

The overall domain alignment loss integrates both local and global discriminators. The local losses are aggregated using the importance weights β_k introduced in the previous section:

$$\mathcal{L}_{\text{domain}}(\{\theta_{D_i}\}, \theta_{D_{\text{global}}}) = \sum_{k=1}^{K} \beta_k \mathcal{L}_{\text{local},k} + \mathcal{L}_{\text{global}}. \tag{10}$$

Maximization of Eq. (16) allows each D_k to focus on aligning its local feature region, while D_{global} ensures that global distribution-level shift is corrected. The adaptive weighting β_k encourages the model to emphasize hard-to-align regions, which often correspond to underrepresented or minority class subdomains.

3.4 Boosted Pairwise Interpolation Generator

To alleviate class imbalance and local domain mismatch, we propose a Boosted Pairwise Interpolation Generator (BPIG) that synthesizes auxiliary samples by interpolating between source-target sample pairs of the same class. These generated samples enhance feature continuity across domains and serve as informative training instances for adversarial alignment.

3.4.1 Generation Trigger

We prioritize sample generation for minority and hard-to-align classes using an adaptive threshold probability P_k for each class k:

$$P_k = \frac{n_k / n_{\max}}{e^{\alpha \cdot w_k}}, \tag{11}$$

where n_k is the number of source samples in class k, $n_{\max}$ is the size of the largest class, w_k is the adaptive weight of class k, and α is a temperature parameter. For each sample in class k, a uniform random variable $r \sim \mathcal{U}(0, 1)$ is generated. The sample is selected for interpolation if $r > P_k$,

A smaller P_k indicates that class k is underrepresented or harder to align, thus increasing its chance of triggering interpolation. The rational behind this formulation ensures: (1) Minority classes with smaller n_k naturally yield lower P_k values, thereby enhancing their sampling priority; (2) Classes with higher difficulty (characterized by larger w_k) are also afforded higher priority via exponential scaling. As a result, This mechanism effectively addresses both inter-class imbalance and intra-class variability.

3.4.2 Adaptive Interpolation

For each source sample $\boldsymbol{x}_s$ that triggered generation with label $y_s = k$, we sample a target pseudo-labeled sample $\boldsymbol{x}_t$ with $\hat{y}_t = k$ and generate an interpolated point:

$$\boldsymbol{x}_p = (1 - \lambda)\boldsymbol{x}_s + \lambda \boldsymbol{x}_t, \quad \lambda \sim \text{Beta}(a, b), \tag{12}$$

where λ is drawn from a symmetric Beta distribution defined by two hyperparameters a and b to encourage interpolation near the midpoint while still allowing variance. This sampling strategy implicitly expands the feature support for minority classes and bridges fragmented cross-domain regions.

3.4.3 Adversarial learning-based Exploration

To enhance the informativeness of generated samples, we formulate a bi-level adversarial optimization to search for the optimal λ^* to explore the hard region. The outer optimization minimizes classification loss over generated samples:

$$\mathcal{L}_{\text{BPIG}}(\theta_f, \theta_g) = -\log \sigma_k(f(g(\boldsymbol{x}_p))), \tag{13}$$

where k is the class index and $\sigma_k(\cdot)$ denotes the predicted probability for class k.

Simultaneously, the inner optimization maximizes the same loss by perturbing the interpolation coefficient λ:

$$\lambda^* = \arg \max_{\lambda \sim \text{Beta}(a,b)} \left[-\log \sigma_k(f(g((1-\lambda)\boldsymbol{x}_s + \lambda \boldsymbol{x}_t))) \right], \tag{14}$$

encouraging the generation of harder samples near the decision boundary. This iteration process of adversarial interplay ensures that the interpolated samples are both realistic and challenging.

3.5 Total Objective Function

The overall training objective integrates multiple loss components to balance classification accuracy, domain alignment, and robustness to class imbalance. It consists of three key parts:

Supervised loss on labeled source samples to ensure basic classification capability:

$$\mathcal{L}_{\text{cls}}(\theta_f, \theta_g) = -\frac{1}{N_s} \sum_{i=1}^{N_s} \sum_{c=1}^{C} y_i^s(c) \log(f(g(\boldsymbol{x}_i^s))(c)) \tag{15}$$

where $y_i^s(c)$ is the one-hot label of source sample i (1 if class c, else 0), and $f(g(\boldsymbol{x}_i^s))(c)$ is the classifier's predicted probability for class c.

To reduce source-target distribution gaps, we minimize the domain discrimination loss:

$$\mathcal{L}_{\text{domain}}(\{\theta_{D_i}\}, \theta_{D_{\text{global}}}) = \sum_{k=1}^{K} \beta_k \mathcal{L}_{\text{local},k} + \mathcal{L}_{\text{global}} \tag{16}$$

To enhance robustness via interpolated samples:

$$\mathcal{L}_{\text{BPIG}}(\theta_f, \theta_g) = \mathcal{L}_{\text{CE}}(\hat{x}_p, y; \theta_g, \theta_f) \tag{17}$$

where θ_g represents the parameters of the feature extractor g, and θ_f denotes the parameters of the classifier f.

The total objective function is a weighted combination of these losses:

$$\min_{(\theta_f, \theta_g)} \max_{(\{\theta_{D_i}\}, \theta_{D_{\text{global}}})} = \lambda_1 \mathcal{L}_{\text{cls}} + \lambda_2 \mathcal{L}_{\text{domain}} + \lambda_3 \mathcal{L}_{\text{BPIG}}. \tag{18}$$

4 Experiments

4.1 Datasets and Baselines

The experiment constructs a class-imbalanced cross-domain adaptation benchmark using two vision datasets: OfficeHome (Venkateswara et al., 2017) and Office31 (Saenko et al., 2010). OfficeHome contains 65 object categories and 4 domains: RealWorld , Clipart, Product, and Art. This experiment focuses on RealWorld, Product, Clipart, with 6 cross-domain tasks: RealWorld→Product (Rw→Pr), RealWorld→Clipart (Rw→Cl), Clipart→Product (Cl→Pr), Clipart→RealWorld (Cl→Rw), Product→RealWorld (Pr→Rw), Product→Clipart (Pr→Cl). Office31(Saenko et al., 2010) is a classic object recognition benchmark with 31 categories and 3 domains: Amazon, Webcam, DSLR. Focusing on all 3 domains, 6 tasks are designed: Amazon→Webcam (A→W), Amazon→DSLR (A→D), Webcam→Amazon (W→A), Webcam→DSLR (W→D), DSLR→Amazon (D→A), DSLR→Webcam (D→W).

To simulate the combined challenge of feature and label distribution shifts, we adopt the Reversely-unbalanced Source (RS) + Unbalanced Target (UT) protocol as shown in Fig. 2. Specifically, class imbalance is introduced via Pareto sampling in both domains, with reversed label distributions.

We selected the following Unsupervised Domain Adaptation (UDA) methods as comparative baselines: BSP(Chen et al., 2019), DANN(Ganin et al., 2016), F-DANN(Wu et al., 2019a), MCD(Saito et al., 2018), COAL(Tan et al., 2020), CDAN-E(Long et al., 2018), Sentry(Prabhu et al., 2021), MDD(Zhang et al., 2019), MDD+implicit(Jiang et al., 2020) and MDD+PAT(Shi et al., 2022a).

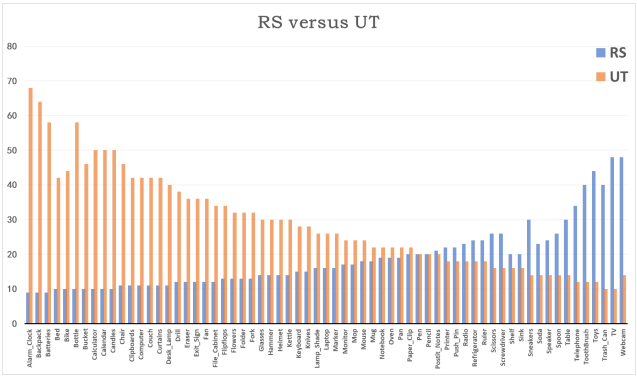

Figure 2: Reversely-unbalanced Source (RS) v.s. Unbalanced Target (UT) protocol.

4.2 Results Analysis

As shown in Table 1, ALFADA consistently outperforms all baselines under the RS→UT protocol on OfficeHome. It achieves an average accuracy of 66.92%, improving upon the strongest baseline (MDD+PAT) by 0.97%. Notably, in Rw→Pr and Pr→Rw, ALFADA yields gains of 1.08% and 1.12%, respectively. Even under large domain gaps (e.g., Rw→Cl), it surpasses prior methods, demonstrating superior adaptability to both domain and label shift. These improvements stem from the framework's integrated mechanisms: adaptive sampling prioritizes informative instances, the local discriminative forest captures regional domain gaps, and boosted interpolation enriches sparse feature manifolds—collectively enabling robust cross-domain adaptation under complex distributional skew.

As shown in Table 2, ALFADA also achieves state-of-the-art results on the Office-31 dataset under the RS→UT protocol, with an average accuracy of 86.63%, surpassing the strongest baseline (MDD+PAT) by 1.34%. The improvements are particularly notable on challenging transfer tasks such as A→W (+1.45%) and A→D (+1.46%), demonstrating the framework's strength in handling both domain and label shift. Even on relatively easier transfers (e.g., W→D and D→W), ALFADA continues to deliver gains, indicating that its adaptive sampling and local discriminative mechanisms provide consistent benefits across varying levels of adaptation difficulty. These results further confirm the generalizability and robustness of ALFADA beyond a single dataset.

To validate the rationality of leveraging per-class MERs to guide the whole training adaptively, we use Figure 3 to visualize the correlation between MER and final classification accuracy on target domains. As MER decreases, corresponding target classification accuracy consistently improves. This trend confirms matching error rate effectively quantifies cross-domain alignment quality. By guiding sampling and alignment during the whole training based on matching error rate, ALFADA rationally focuses on minority instances and bridge domain shift and classification robustness.

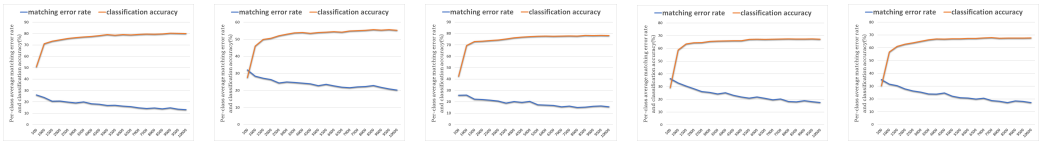

(a) Rw→Pr (b) Rw→Cl (c) Pr→Rw (d) Cl→Rw (e) Cl→Pr

Figure 3: Per-class average matching error rates and the corresponding classification accuracies.

4.3 Ablation Study

To verify the effectiveness of each component in ALFADA, we conduct ablation experiments. We use the DANN as our base model and evaluate Local Discriminative Forest (LDF) and Boosted Pairwise Interpolation Generator (BPIG) by comparing the full model against variants with each component removed. The setup is consistent with our main experiments, using the same dataset

Table 1: Per-class average accuracy (%) on Office-Home dataset with RS→UT label shift.

Method	Rw→Pr	Rw→Cl	Pr→Cl	Pr→Rw	Cl→Rw	Cl→Pr	AVG
BSP	72.74	23.88	20.09	66.26	32.79	30.41	41.03
DANN	71.89	46.05	35.78	68.06	58.69	57.83	56.38
F-DANN	58.56	40.57	37.29	67.32	55.84	53.67	44.24
MCD	66.34	32.19	29.74	62.59	41.47	38.75	45.18
COAL	73.68	42.64	38.16	73.29	59.36	57.27	57.40
CDAN-E	70.85	45.91	36.43	69.83	53.96	54.82	59.07
Sentry	76.14	56.77	48.69	73.62	65.96	64.33	64.25
MDD	71.18	44.75	42.26	69.35	52.12	52.68	55.42
MDD+implicit	76.10	50.08	45.73	74.31	61.11	63.20	61.76
MDD+PAT	79.29	54.63	50.17	77.25	67.21	67.15	65.95
ALFADA(Ours)	**80.37**	**55.71**	**51.41**	**78.37**	**67.69**	**67.98**	**66.92**

Table 2: Per-class average accuracy (%) on Office-31 with RS→UT label shift.

Method	A→W	D→W	W→D	A→D	D→A	W→A	AVG
BSP	71.77	90.86	93.06	72.25	59.03	58.34	74.21
F-DANN	69.83	93.56	93.95	76.45	58.57	58.11	75.07
COAL	81.18	91.12	95.46	81.67	66.08	66.60	80.35
CDAN-E	76.25	95.78	94.85	79.92	64.04	58.69	78.25
Sentry	82.01	90.86	93.73	83.55	62.79	63.88	79.47
MDD	83.99	96.69	96.71	83.94	67.23	61.36	81.65
MDD+implicit	85.79	96.20	97.40	84.25	68.11	66.63	83.06
MDD+PAT	89.61	96.08	97.08	86.66	71.93	70.40	85.29
ALFADA(Ours)	**91.06**	**97.42**	**97.70**	**88.12**	**73.49**	**71.98**	**86.63**

splits, per-class accuracy metric, and hyperparameters. As table 3 illustrated, removing the Local Discriminative Forest will cause performance drops across all tasks, with the most significant declines in Rw→Cl (will drop by 0.99%) and Cl→Pr (will drop by 0.97%). This indicates LDF's role in capturing fine-grained regional discrepancies, critical for aligning sparse minority features overlooked by global alignment. Removing BPIG will lead to an average drop of 4.76% due to the reason that BPIG enriches sparse regions via source-target interpolations, enhancing decision boundary robustness for underrepresented classes. These results demonstrate Local Discriminative Forest enables fine-grained alignment, and BPIG enriches sparse regions, collectively addressing class imbalance and domain shift.

Table 3: Per-class average accuracy(%) of DANN, ALFADA w/o BPIG, ALFADA w/o Local Discriminative Forest(LDF), and ALFADA (full) on imbalanced Office-Home dataset.

Method	Rw→Pr	Rw→Cl	Pr→Cl	Pr→Rw	Cl→Rw	Cl→Pr	AVG
DANN	71.89	46.05	35.78	68.06	58.69	57.83	56.38
ALFADA w/o BPIG	76.8	51.03	41.39	72.54	66.21	64.97	62.16
ALFADA w/o LDF	78.89	54.72	48.12	77.95	66.97	67.01	65.61
ALFADA (full)	**80.37**	**55.71**	**51.41**	**78.37**	**67.69**	**67.98**	**66.92**

5 CONCLUSION

In this paper, we propose ALFADA, a novel adversarial domain adaptation framework tailored for scenarios with severe class imbalance and label distribution shift. By leveraging adaptive instance weighting based on matching error rates, constructing a local discriminative forest for region-specific alignment, and generating interpolated samples via a Boosted Pairwise Interpolation Generator (BPIG), ALFADA effectively addresses both global and local domain discrepancies. Extensive experiments on the Office-Home and Office-31 benchmarks demonstrate that ALFADA consistently outperforms state-of-the-art methods across all transfer tasks.

REFERENCES

Roberto Alcover-Couso, Marcos Escudero-Viñolo, Juan C SanMiguel, and Jesus Bescos. Gradient-based class weighting for unsupervised domain adaptation in dense prediction visual tasks. *Pattern Recognition*, 166:111633, 2025.

Atif Belal, Akhil Meethal, Francisco Perdigon Romero, Marco Pedersoli, and Eric Granger. Attention-based class-conditioned alignment for multi-source domain adaptation of object detectors. In *Proceedings of the IEEE/CVF Winter Conference on Applications of Computer Vision (WACV)*, 2025.

Xinyang Chen, Sinan Wang, Mingsheng Long, and Jianmin Wang. Transferability vs. discriminability: Batch spectral penalization for adversarial domain adaptation. In *International conference on machine learning*, pp. 1081–1090. PMLR, 2019.

Yaroslav Ganin and Victor Lempitsky. Domain-adversarial training of neural networks. In *Journal of Machine Learning Research*, 2016.

Yaroslav Ganin, Evgeniya Ustinova, Hana Ajakan, Pascal Germain, Hugo Larochelle, François Laviolette, Mario March, and Victor Lempitsky. Domain-adversarial training of neural networks. *Journal of Machine Learning Research*, 17(59):1–35, 2016. URL `http://jmlr.org/papers/v17/15-239.html`.

Dandan Guo, Zhuo Li, Meixi Zheng, He Zhao, Mingyuan Zhou, and Hongyuan Zha. Learning to re-weight examples with optimal transport for imbalanced classification. In *Advances in Neural Information Processing Systems (NeurIPS)*, 2022.

Bin Huang, Lin Ding, Jiayi Zhou, et al. Gradient-based dynamic reweighting for class-imbalanced semantic segmentation. *arXiv preprint arXiv:2407.01327*, 2023.

Jiaxing Huang, Dayan Guan, Aoran Xiao, Shijian Lu, and Ling Shao. Category contrast for unsupervised domain adaptation in visual tasks. In *Proceedings of the IEEE/CVF Conference on Computer Vision and Pattern Recognition (CVPR)*, pp. 1203–1213, 2022.

Xiang Jiang, Qicheng Lao, Stan Matwin, and Mohammad Havaei. Implicit class-conditioned domain alignment for unsupervised domain adaptation. In *International conference on machine learning*, pp. 4816–4827. PMLR, 2020.

Shengjie Liu, Chuang Zhu, Yuan Li, and Wenqi Tang. Wuda: Unsupervised domain adaptation based on weak source domain labels. In *ICASSP 2023-2023 IEEE International Conference on Acoustics, Speech and Signal Processing (ICASSP)*, pp. 1–5. IEEE, 2023a.

Yang Liu, Zhipeng Zhou, and Baigui Sun. Cot: Unsupervised domain adaptation with clustering and optimal transport. In *Proceedings of the IEEE/CVF conference on computer vision and pattern recognition*, pp. 19998–20007, 2023b.

Mingsheng Long, Zhangjie Cao, Jianmin Wang, and Michael I Jordan. Conditional adversarial domain adaptation. *Advances in neural information processing systems*, 31, 2018.

Takeru Miyato, Shin-ichi Maeda, Masanori Koyama, and Shin Ishii. Virtual adversarial training: a regularization method for supervised and semi-supervised learning. In *IEEE TPAMI*, 2018.

Zhongyi Pei, Zhangjie Cao, Mingsheng Long, and Jianmin Wang. Multi-adversarial domain adaptation. In *Proceedings of the AAAI conference on artificial intelligence*, volume 32, 2018.

Vishal Prabhu, Mitesh M Birla, Tengyu Ma, and Sriram Ravi. Sentry: Selective entropy optimization via committee consistency for unsupervised domain adaptation. In *ICML*, 2021.

Kate Saenko, Brian Kulis, Mario Fritz, and Trevor Darrell. Adapting visual category models to new domains. In *European conference on computer vision*, pp. 213–226. Springer, 2010.

Kuniaki Saito, Kohei Watanabe, Yoshitaka Ushiku, and Tatsuya Harada. Maximum classifier discrepancy for unsupervised domain adaptation. In *Proceedings of the IEEE conference on computer vision and pattern recognition*, pp. 3723–3732, 2018.

Weili Shi, Ronghang Zhu, and Sheng Li. Pairwise adversarial training for unsupervised class-imbalanced domain adaptation. In *Proceedings of the 28th ACM SIGKDD conference on knowledge discovery and data mining*, pp. 1598–1606, 2022a.

Zhihao Shi et al. Pat: Pairwise adversarial training for deep unsupervised domain adaptation. In *ICML*, 2022b.

Rui Shu, Hung H Bui, Hirokazu Narui, and Stefano Ermon. A dirt-t approach to unsupervised domain adaptation. *arXiv preprint arXiv:1802.08735*, 2018.

Shuhan Tan, Xingchao Peng, and Kate Saenko. Class-imbalanced domain adaptation: An empirical odyssey. In *European Conference on Computer Vision*, pp. 585–602. Springer, 2020.

Hemanth Venkateswara, Jose Eusebio, Shayok Chakraborty, and Sethuraman Panchanathan. Deep hashing network for unsupervised domain adaptation. In *Proceedings of the IEEE conference on computer vision and pattern recognition*, pp. 5018–5027, 2017.

Yinong Oliver Wang, Younjoon Chung, Chen Henry Wu, and Fernando De la Torre. Domain gap embeddings for generative dataset augmentation. In *Proceedings of the IEEE/CVF Conference on Computer Vision and Pattern Recognition (CVPR)*, pp. 28684–28694, 2024.

Yifan Wu, Ezra Winston, Divyansh Kaushik, and Zachary Lipton. Domain adaptation with asymmetrically-relaxed distribution alignment. In *International conference on machine learning*, pp. 6872–6881. PMLR, 2019a.

Zuxuan Wu, Xin Wang, Joseph E Gonzalez, Tom Goldstein, and Larry S Davis. Ace: Adapting to changing environments for semantic segmentation. In *Proceedings of the IEEE/CVF international conference on computer vision*, pp. 2121–2130, 2019b.

Yuchen Zhang, Tianle Liu, Mingsheng Long, and Michael Jordan. Bridging theory and algorithm for domain adaptation. In *International conference on machine learning*, pp. 7404–7413. PMLR, 2019.